Journal of Molecular Spectroscopy **203,** 188–195 (2000)
doi:10.1006/jmsp.2000.8165, available online at http://www.idealibrary.com on IDEAL®

Fourier Transform Spectroscopy of Chemiluminescence from the SrO $A^1\Sigma^+$–$X^1\Sigma^+$ Transition

Hongzhi Li, Randall Skelton, Cristian Focsa,[1] Bernard Pinchemel,[1] and Peter F. Bernath

Department of Chemistry, University of Waterloo, Waterloo, Ontario, Canada N2L 3G1

Received April 17, 2000

The $A^1\Sigma^+$–$X^1\Sigma^+$ chemiluminescence spectrum of SrO was observed using a Fourier transform spectrometer. SrO was produced in a Broida-type oven from the Sr + N_2O reaction. A total of 75 bands from ^{88}SrO, ^{87}SrO, and ^{86}SrO were measured in the range of 7600–13 600 cm^{-1} at a resolution of 0.04 cm^{-1}. The vibrational levels of the ground state were observed up to $v'' = 12$ and over 10 000 rovibrational lines with J as high as 153 were analyzed at a precision of about 0.005 cm^{-1}. Significantly improved spectral constants for the ground state were obtained by representing the perturbed excited state by term values and by adding the known microwave data and infrared data to our fit. Strong perturbations were observed in the upper A state. The vibrational levels of the $A^1\Sigma^+$ state were measured up to $v' = 8$ and some new perturbations are reported.

I. INTRODUCTION

The first studies of the spectra of strontium oxide in the gas phase were carried out long ago. Mecke and Guillery (*1*) obtained some blue bands belonging to the $B^1\Pi$–$X^1\Sigma^+$ transition in 1928. Later, Querbach (*2*), Mahla (*3*), and Meggers (*4*) studied the $A^1\Sigma^+$–$X^1\Sigma^+$ bands in various spectral regions. Starting in 1949, Lagerqvist and co-workers (*5–7*) rotationally analyzed 10 bands in the $A^1\Sigma^+$–$X^1\Sigma^+$ transition of ^{88}SrO. The vibrational levels of the ground state were observed up to 5, and those of the A state up to 4. The maximum rotational quantum number detected was up to $J = 123$ in the (1, 0) band (*6*).

Pure rotational data for the ground state were first reported in 1965 by Kaufman *et al.* (*8*) using the molecular beam electric resonance method. Hocking *et al.* (*9*) measured the millimeter-wave spectra of SrO using a Broida-type oven for 11 transitions with J values up to 10. Blom *et al.* (*10*) performed new microwave measurements for SrO using a Flygare–Balle molecular beam spectrometer. They observed the $J = 1 \leftarrow 0$ transition for $v'' = 0$ to 6 and also obtained the first high-resolution infrared spectrum of SrO between 618 and 666 cm^{-1}. A total of 43 lines from three isotopomers, i.e., ^{88}SrO, ^{87}SrO, and ^{86}SrO, were measured with a diode–laser spectrometer. The spectral constants derived by Blom *et al.* are the best so far for the ground state.

Lagerqvist *et al.* (*5, 6*) found numerous strong perturbations in the $A^1\Sigma^+$ state. Field (*11*) reinterpreted the data and attributed the perturbations to interactions between the $A^1\Sigma^+$ state and the $A'^1\Pi$ state as well as with the three spin components of the $a^3\Pi_i$ state. Later, Capelle *et al.* (*12*) measured the A'–X chemiluminescence at a low resolution and obtained improved molecular constants for the $A'^1\Pi$ state. In Field's work (*11*), there was an ambiguity of one unit in the vibrational numbering of the $A'^1\Pi$ state that was resolved by recording a low-resolution spectrum of the A'–X transition for Sr^{18}O isotopomer (*13*). As part of our recent work on CaO, SrO, and BaO, we have also recorded the A'–X emission spectrum at a resolution of 0.03 cm^{-1} between 4000 and 10 000 cm^{-1}, but this work will be reported elsewhere (*14*). Direct observation of the low-lying $a^3\Pi$ and $b^3\Sigma^+$ triplet states was made by Herrmann *et al.* by high-resolution laser excitation spectroscopy of the orange band systems (*15*).

We report on a reanalysis of the $A^1\Sigma^+$–$X^1\Sigma^+$ transition of SrO between 7800 and 13 330 cm^{-1} using a Fourier transform spectrometer to obtain improved spectroscopic constants for the ground state. In this first stage of the analysis, we represented the excited state entirely by a set of term values in our fits. In this way, our ground state constants are not affected by the extensive strong perturbations in the excited state. Over 10 000 rovibrational lines from ^{88}SrO, ^{87}SrO, and ^{86}SrO were analyzed. Significantly improved spectral constants were obtained by fitting our new data together with the microwave and infrared data from the literature.

II. EXPERIMENT

The SrO chemiluminescence was generated in a Broida-type oven (*16, 17*) by the reaction of strontium vapor with nitrous oxide. The strontium metal was heated in an alumina crucible

Supplementary data for this article are available on IDEAL (http://www.idealibrary.com) and as part of the Ohio State University Molecular Spectroscopy Archives (http://msa.lib.ohio-state.edu/jmsa_hp.htm).

[1] Permanent address: Laboratoire de Physique des Lasers, Atomes et Molécules, UMR CNRS 8523, Centre d'Etudes et de Recherches Lasers et Applications, Université des Sciences et Technologies de Lille, 59 655 Villeneuve d'Ascq Cedex, France.

0022-2852/00 $35.00

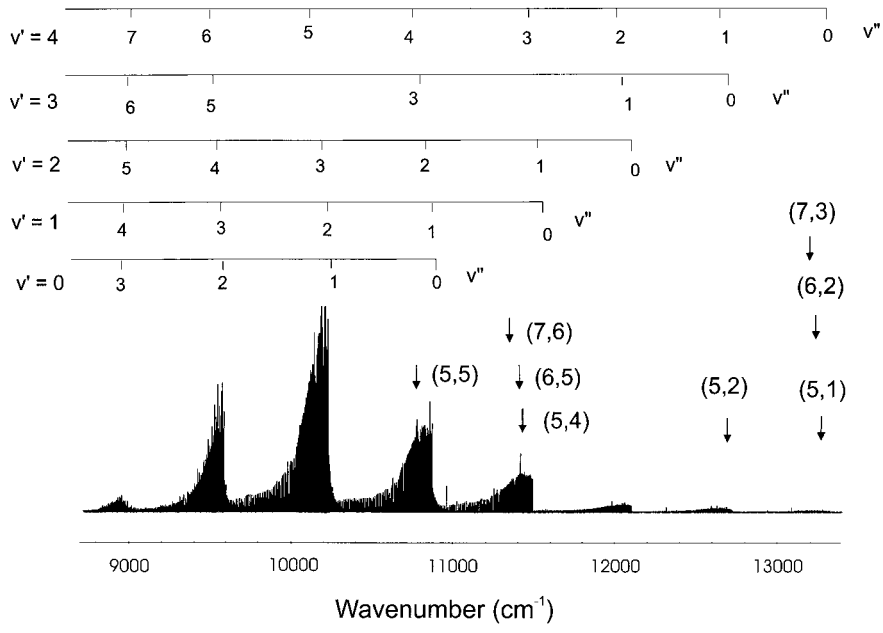

FIG. 1. The SrO chemiluminescence spectrum in the range of 8800–13 500 cm^{-1} obtained with a Si photodiode detector. Most lines are from the $A^1\Sigma^+$–$X^1\Sigma^+$ transition. Some vibrational assignments for the A–X transition are labeled in the figure.

by a tungsten wire basket heater with a current of about 40 A. The vaporized strontium was carried out of the crucible by a flow of argon gas and then mixed with nitrous oxide in the reaction chamber. The argon pressure was maintained at about 5 Torr. A low-pressure chemiluminescent flame was produced by the exothermic reaction of Sr with N_2O (*10, 18*). The partial pressures of Ar and N_2O were adjusted separately to optimize the flame intensity.

The chemiluminescence was focused into a Bruker IFS 120 HR Fourier transform spectrometer. The spectrometer was modified to measure double-sided interferograms to improve the lineshape. In one of our experiments, a silicon photodiode detector was employed to measure the spectrum in the 8000–15 000 cm^{-1} range. A red-pass filter (<16 000 cm^{-1}) was used to eliminate the high-wavenumber emission, and a notch filter (blocking range of 15 500–15 850 cm^{-1}) was used to reduce the strong He–Ne laser signal. The resolution was set to 0.04 cm^{-1} and 30 scans were co-added to obtain the spectrum shown in Fig. 1. For calibration purposes, an argon pen lamp was lit for about 3 min during the experiment to record several argon atomic emission lines. In another experiment, we used a liquid-nitrogen-cooled InSb detector to record the spectrum between 5300 and 10 000 cm^{-1}. A blue-pass filter (>5000 cm^{-1}) was used and the resolution was 0.03 cm^{-1}. A total of 100 scans were co-added to obtain a good signal-to-noise ratio, as shown in Fig. 2.

The line positions were measured by a Microsoft Windows-based program called WSpectra, written by Dr. Michel R. Carleer (Laboratoire Chimie Physique Moléculaire, Université Libre de Bruxelles, Belgium). Voigt lineshape functions were used in a nonlinear least-squares fitting of the peaks. To generate enough points for a good fit of the dense regions of the spectrum, a zero-filling factor of 8 had to be used. In preliminary measurements, there were problems fitting overlapping lines when the zero-filling factor was only 2.

The air-to-vacuum conversion of the line positions was

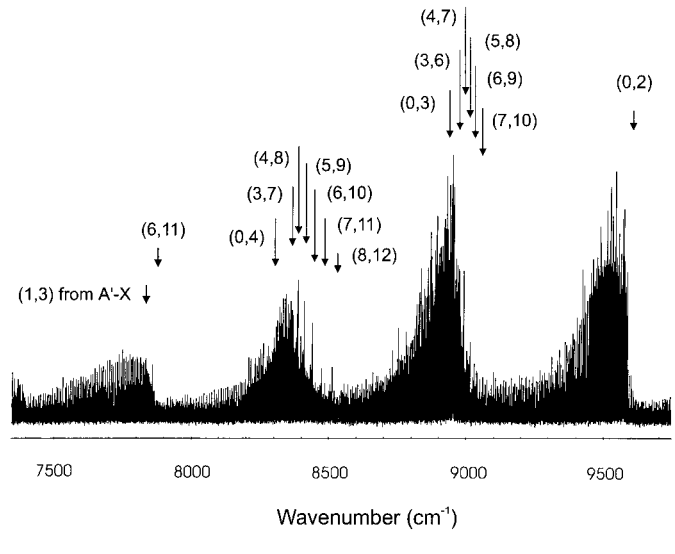

FIG. 2. The SrO emission spectrum in the near-infrared obtained with an InSb detector. Some of the bands belonging to the A–X transition are shown, with v' up to 8 and v'' up to 12 for the (8, 12) band. Most of the A–X bands suddenly disappear below 8000 cm^{-1}, where the bands from the $A'^1\Pi$–$X^1\Sigma^+$ transition become stronger. The (1, 3) band from the A'–X transition can be seen in the low wavenumber region.

carried out with an equation developed by Dr. Tsuyoshi Hirao in this laboratory (*19*). His derivation was based on the Edlén's formula (*20, 21*) for the refractive index of air. For the spectrum from the Si photodiode detector, the calibration factor was obtained by measuring the argon atomic line positions in the spectrum (*22*). Four Ar lines in the range of 10 950–13 100 cm^{-1} were used to yield a calibration factor of 1.000002621215. The other spectrum, recorded with the InSb detector, was calibrated onto the same wavenumber scale using common lines in the two spectra. About 100 common lines from the (0, 2) band, covering a range of 9000 to 9481 cm^{-1}, were used to obtain a calibration factor of 1.000002743687 for the second spectrum. The precision of our final measurements was estimated to be about 0.005 cm^{-1} for medium strength, unblended lines.

TABLE 1

A List of the Rotationally Assigned Bands for the $A^1\Sigma^+$–$X^1\Sigma^+$ Chemiluminescence Spectrum of SrO, Including 53 Bands of ^{88}SrO, 10 Bands of ^{87}SrO, and 12 Bands of ^{86}SrO

v′ \ v″	0	1	2	3	4	5	6	7	8	9	10	11	12
0	abc	abc	abc	a	a								
1	abc	a	abc	abc	abc	a							
2	abc	a	ac	a	ac	a	a						
3	a	abc		abc		a	a	a					
4	a	a	a	a	a	a	a	a	a				
5		a	a		a	a	a	a	a	a			
6			a			a		a		a	a	a	
7				a			a				a	a	
8												a	a

a: Analyzed band of ^{88}SrO
b: Analyzed band of ^{87}SrO
c: Analyzed band of ^{86}SrO

III. RESULTS AND DISCUSSION

$A^1\Sigma^+$–$X^1\Sigma^+$ bands and $A'^1\Pi$–$X^1\Sigma^+$ bands are mixed together in our chemiluminescence spectra, but in the region of 8000–14 000 cm^{-1}, the *A*–*X* transition dominates. In the region below 8000 cm^{-1}, *A*′–*X* transitions are extremely strong, while the *A*–*X* bands disappear. This paper focuses on the *A*–*X* emission, while Skelton *et al.* (*14*) will present our analysis of the *A*′–*X* chemiluminescence in another paper.

Figure 1 shows the spectrum measured with the photodiode detector. The (0, 3) band, which is at the lower wavenumber end of the spectrum, is weaker than in the spectrum recorded with InSb detector, as shown in Fig. 2. In the end, the lines for the (0, 2) band (Fig. 1) were taken from the photodiode spectrum, while the (0, 3) lines came from the InSb spectrum (Fig. 2) in our analysis. The (1, 3) band from the *A*′–*X* transition can be clearly seen around 7850 cm^{-1} (Fig. 2). Many more *A*′–*X* bands were observed below 7500 cm^{-1} and are not shown in Fig. 2. No lines were found below 7800 cm^{-1} that belonged to the *A*–*X* transition.

A. Vibrational Analysis

Most of the strong bands shown in the figures can be vibrationally assigned using the best available spectral constants for both states from Refs. (*10*) and (*11*). The discrepancies between the predicted bandhead positions and our experimental results are typically several wavenumbers. However, the weak and blended bands could not be assigned in this way because of the inaccuracy of the spectral constants and the strong perturbations in the *A* state. The best way to vibrationally assign a band is to perform a rotational analysis, as discussed in detail in the next section.

Some of the vibrational assignments are shown in Figs. 1 and 2. The (0, 1) band, with a head at 10 226.12 cm^{-1}, is the strongest band in our measurements. Two other bands with $v' = 0$, i.e., (0, 0) band with a head at 10 871.51 cm^{-1} and (0, 2) band at 9588.65 cm^{-1}, are also very strong. The (4, 0) band with a head at 13 328.5 cm^{-1} is the band with the highest wavenumber in our observations. Three other bands, i.e., (5, 1) at 13 289.1 cm^{-1}, (6, 2) at 13 256.1 cm^{-1}, and (7, 3) whose head is hard to distinguish, are also found in this v'–$v'' = 4$ sequence.

As shown in Fig. 2, the band with the smallest wavenumber head is (6, 11) with a head at 7875.3 cm^{-1}. However, the heads of two other bands with lower wavenumbers, i.e., (4, 9) around 7806 cm^{-1} and the (5, 10) band at 7,837.2 cm^{-1}, can be distinguished but no rotational analysis was carried out. Among the analyzed bands, the highest vibrational quantum number for the *X* and *A* states was found for the (8, 12) band, i.e., the highest v' is 8 and the highest v'' is 12. We also observed the (9, 13) band with a head at 8555.8 cm^{-1} and the (10, 14) band around 8602 cm^{-1} but without detailed analysis. The most congested region is around 8500 cm^{-1}, where numerous bands with v' from 0 to 10 and $\Delta v = 4$ are observed.

In a total, 53 bands for ^{88}SrO, 10 bands for ^{87}SrO, and 12 bands for ^{86}SrO were rotationally assigned, and they are listed in Table 1.

B. Rotational Assignment for ^{88}SrO

Due to the much stronger perturbations in the $A^1\Sigma^+$ state of SrO than for the $A^1\Sigma^+$ state of BaO, we adopted a different procedure for the rotational analysis of the SrO data than we used for our previous work on BaO (*23*). For example, the Loomis program, written by Dr. C. Jarman, using the method developed by Loomis and Wood (*24*) to pick out of branches for unperturbed bands, was not as useful for SrO as for BaO. However, the Loomis program was still helpful in picking out lines in the weakly perturbed parts of a band. Furthermore, because the program displays the relative intensity of lines using different colors, the perturbed lines in a branch could sometimes be followed.

Lagerqvist and co-workers (*5–7*) rotationally assigned the (0, 0), (0, 2), (1, 0), (1, 3), (2, 0), (2, 4), (3, 0), (3, 1), (3, 5), and (4, 1) bands of ^{88}SrO, which gave us a good start for our

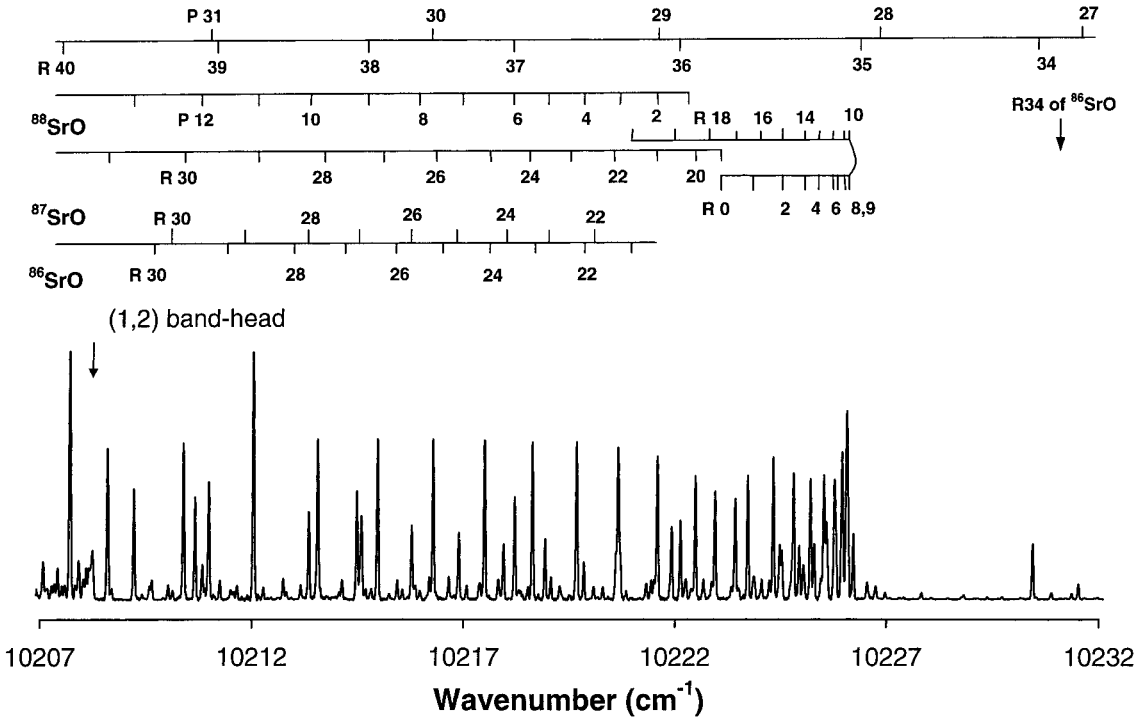

FIG. 3. Rotational assignment of the (0, 1) band near the bandhead. For ^{88}SrO, a perturbation can be seen near $R(20)$. Two series of extra lines, assigned from $P(31)$ to $P(27)$ and from $R(40)$ to $R(34)$, extend across the center of the band and even go beyond the bandhead. Several lines from the ^{87}SrO and ^{86}SrO isotopomers are also shown. The head of the weaker (1, 2) band can be seen in the low wavenumber region.

rotational assignments. The line positions that they published are close to our data, with an average discrepancy of only about 0.05 cm^{-1}. However, the discrepancies of several lines were as large as 0.6 cm^{-1}. For example, the position for the $R(112)$ line in the (0, 0) band was measured to be 10 561.987 cm^{-1} in our spectrum, while it was reported as 10 561.36 cm^{-1} in Ref. (*6*).

Because the upper state is strongly perturbed, it was impossible for us to assign the rotational lines by calculation using the known spectral constants. Taking advantage of the unperturbed nature of the ground state, we based our assignments on ground state combination differences:

$$\Delta_2 F''(J) = F_v(J+1) - F_v(J-1) \approx 4B_v(J+1/2) - 8D_v(J+1/2)^3. \quad [1]$$

This relationship was also used to predict the line positions of one branch, provided the other branch has been assigned. However, using only combination differences in a dense spectral region is a recipe for disaster. A huge number of potential *P–R* doublet pairs could satisfy Eq. [1], and it is almost impossible to pick out the correct assignment from the numerous candidates. Some other methods need to be used to reduce the number of candidates. For example, sometimes it was helpful to follow the intensity pattern of a branch manually or by using the Loomis program.

Another assignment method played an important role in this work. For a vibrational progression (v', v'') from the same excited state v', if one band for a specific v''_{ass} has been assigned, then the line positions of the other bands in the progression can be predicted reliably. Provided that there are no perturbations in the ground state, the positions of the other bands (v', v'') can be calculated from the known band (v', v''_{ass}), using the relationship:

$$F_{v''}(J) - F_{v''_{ass}}(J) \approx G_{v''} - G_{v''_{ass}} + (B_{v''} - B_{v''_{ass}})J(J+1) - (D_{v''} - D_{v''_{ass}})J^2(J+1)^2. \quad [2]$$

When one band in a progression was assigned, the other bands were all assigned using the predicted positions from Eq. [2]. Furthermore, when there were several bands belonging to the same progression and none of them were assigned, applying both Eqs. [1] and [2] proved to be useful, as described in our previous BaO work (*23*). Most of the bands with $v' > 4$ were assigned in this way.

Accurate spectral constants are needed when employing Eq. [2] to analyze dense spectra. The best available ground state constants, from Ref. (*10*), were found to be useful for bands with low v'' or low J. For example, when we used the (4, 0) band to predict the (4, 5) band, using Blom *et al.*'s constants, the discrepancy of a calculated line position was about 0.06

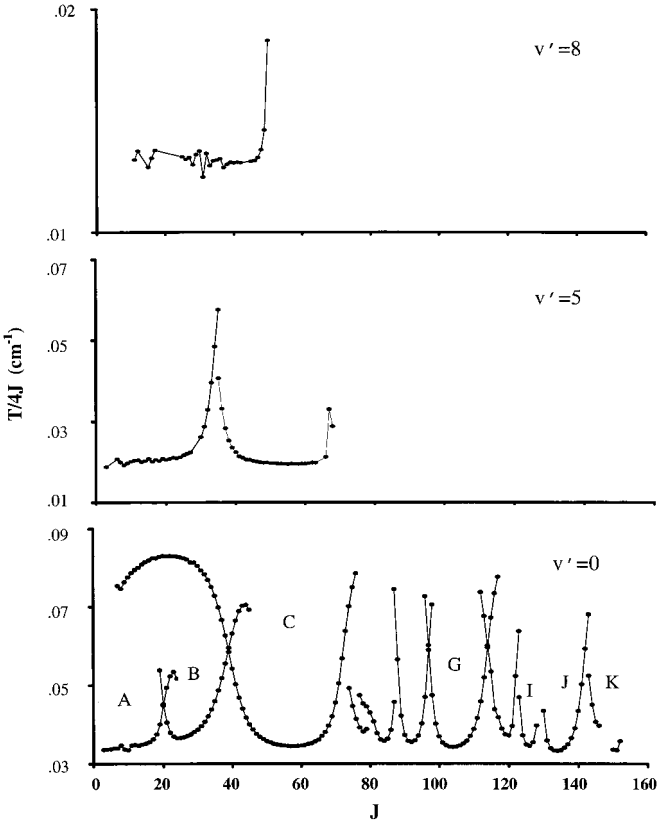

FIG. 4. A Gerö plot of $T/4J$ against J to show the perturbations in the $A^1\Sigma^+$ state of ^{88}SrO. The vibrational levels with $v' = 0$, $v' = 5$, and $v' = 8$ are displayed. Each series of lines is marked as *A*, *B*, etc., to distinguish them in the $v' = 0$ plot.

cm^{-1} for $J \approx 50$. The discrepancy becomes as large as 0.8 cm^{-1} for $J \approx 50$ for the (4, 8) band. This is not surprising because the constants of Blom *et al.* (*10*) were derived from the data of relatively low J and v. So, we only used their constants at the beginning of our assignment to predict the low v'' bands. We gradually revised the ground state constants, using the higher v'' and higher J data, and eventually we reached $v'' = 12$.

Figure 3 shows a part of the rotational assignment of the (0, 1) band. The bandhead is assigned as the overlap of the $R(8)$, $R(9)$, and $R(10)$ lines. $R(0)$ can be clearly distinguished at 10 223.555 cm^{-1}, while $P(1)$ is at 10 222.300 cm^{-1}. Strong perturbations can be seen throughout the region and are discussed in next section. Some lines from ^{87}SrO and ^{86}SrO are also assigned, as discussed in Section D. The bandhead of the (1, 2) band at 10 208.30 cm^{-1}, which occurs at the $R(9)$ and $R(10)$ lines, is also marked in the figure.

A total of 9047 rovibrational lines were assigned. The maximum J'' observed is 153 in the (0, 1) and (0, 0) bands, compared to J_{max} of 123 as reported in Almkvist and Lagerqvist's paper (*6*). We also observed many new extra lines that result from perturbations. For example, as shown in Fig. 3, the extra lines that are beyond the bandhead, like $R(34)$, are newly assigned. All these assignments, together with about 1000 lines from minor isotopomers, are available electronically. An additional letter is added to the assignment to distinguish between the different series of perturbed lines in a band.

C. Perturbations

Strong perturbations were observed in the $A^1\Sigma^+$ state of ^{88}SrO. The value of $T/4J$ defined by Gerö (*25*) as

$$T/4J = [R(J-2) - R(J-1) + P(J) - P(J+1)]/4J \approx B'' - B' + 6D'' - 2J^2(D'' - D') \quad [3]$$

is used to show the perturbations in Fig. 4. In unperturbed regions, the $T/4J$ vs. J plot should be roughly a horizontal line with a constant value of about $B'' - B' + 6D''$, if $D'' \approx D'$. The $T/4J$ value changes if a perturbation occurs, as illustrated in Fig. 4 for three vibrational levels in the A state.

In Fig. 4, the plot with $v' = 8$ is from the (8, 12) band. One perturbation can be seen around $J = 50$, where the $T/4J$ values deviate from a horizontal line. The value of B''–B' is about 0.013 cm^{-1} for the unperturbed part. The plot with $v' = 5$ is from the (5, 8) band. One perturbation around $J = 35$ and another with $J > 67$ were observed. The value of B''–B' is about 0.021 cm^{-1} in this band.

The $T/4J$ plot for $v' = 0$ of the A state in Fig. 4 is from the (0, 0) band. Perturbations can be seen every few J values. For example, as shown in Fig. 3, a perturbation can be clearly seen around $R(20)$. We use a letter to mark each series of lines to distinguish them in the figure. We adopted the same letter for our rotational assignment in the electronic line list. For example, the first series of lines starting at $J = 2$ is marked as the "A" series. Thus the $P(J)$ line in this series is assigned as $Pa(J)$ in our analysis. Similarly, $Rc(J)$ in our assignment means a $R(J)$ line in the "C" perturbed series. This labeling method simplified the handling of the data by our computer programs and is also convenient for discussion.

We observed all of the perturbations published in Ref. (*6*) for the (0, 0) band. We also measured more lines with higher J quantum numbers and the I, J, and K series in Fig. 4 with $J > 123$ are all newly observed. Furthermore, we obtained more extra lines for the low J region. For example, the lines of the perturbed series C in Fig. 4 with $J < 32$ are also new. The shape of the C series in Fig. 4 is very interesting. When $J < 30$, the $T/4J$ plot is close to a horizontal line again, but with a larger value. These lines are in fact from $v = 4$ of the $a^3\Pi_0$ spin component present because of perturbation mixing. In Fig. 3, the assigned series labeled on the top from $R(40)$ to $R(34)$ are actually from the perturbed series C. The perturbation is so strong that starting from $R(35)$ and $P(28)$, the perturbed lines are beyond the bandhead. The $Rc(5)$ line was observed at 10 951.471 cm^{-1}, which is about 80 cm^{-1} blue-shift from the $Ra(5)$ line. The crossing of the C series through the bandhead

TABLE 2
Observed Perturbations and the Vibronic Assignments

$A^1\Sigma(v)$	$A'^1\Pi(v)$	$a^3\Pi_2(v)$	$a^3\Pi_1(v)$	$a^3\Pi_0(v)$	Observed J_0	$A^1\Sigma(v)$	$A'^1\Pi(v)$	$a^3\Pi_2(v)$	$a^3\Pi_1(v)$	$a^3\Pi_0(v)$	Observed J_0
0			4		20	2				8	102
0				4	39	2	8				119
0	4				72	2		9			119*
0		5			81	2			9		124
0			5		88	2				9	~130
0				5	97						
0	5				114	3				8	9
0		6			~116	3	8				63
0			6		122	3			9		76
0				6	129	3				9	85
0	6				142	3	9				104
0		7			142*	3		10			104*
0			7		148	3			10		111
0				7	~152	3				10	~119
1	5				47	4	9				30
1		6			59	4		10			~43
1			6		68	4			10		52
1				6	80	4				10	65
1	6				100	4	10				89
1		7			~104	4		11			89*
1			7		110	4			11		97
1				7	117						
1	7				130	5				11	35
1		8			130*	5	11				>67
1			8		136						
1				8	~142**	6	12				45
						6			13		>56
2			7		~44						
2				7	57	7				14	~41
2	7				83						
2		8			~88	8	15				>50
2			8		94						

* The $A^1\Sigma^+$–$a^3\Pi_2$ perturbations tend to be weak and coincidentally overlapped with the strong $A^1\Sigma^+$–$A'^1\Pi$ perturbation.
** Perturbation is determined only by the R-branch.

causes the heads of bands with $v' = 0$ to be fuzzy in a compressed spectrum such as Fig. 1.

The perturbations result from the interactions of the $A^1\Sigma^+$ state with the $A'^1\Pi$ state and the three spin components of the $a^3\Pi_i$ state (*11*). The perturbations we observed and their interaction partners are listed in Table 2. We are contemplating a full perturbation analysis.

D. Isotopomers

The three major isotopes of Sr have natural abundances of 82.58% for ^{88}Sr, 7.00% for ^{87}Sr, and 9.86% for ^{86}Sr. Most of the rovibrational lines of ^{87}SrO and ^{86}SrO can be easily picked out using the Loomis program. For heavy diatomic molecules such as SrO, ignoring perturbations, the branches from the minor isotopomers can be clearly seen as parallel lines near the main ^{88}SrO isotopomer in the Loomis program (*23*). Most of the lines from ^{87}SrO and ^{86}SrO were found and assigned in this way. Some minor isotopomer lines are shown in Fig. 3.

However, due to strong perturbations in the *A* state, many of the minor isotopomer lines were difficult to find. For example, the *P*b(38) line (see section C for the perturbation series tag "b") of ^{88}SrO is 0.13 cm^{-1} higher than that of ^{87}SrO and 0.28 cm^{-1} higher than that of ^{86}SrO. For the lower *J* lines in the same perturbed series, the difference between the main isotopomer and minor isotopomers increased dramatically, then decreased, and eventually became erratic. For example, the *P*b(27) line of ^{88}SrO is 0.47 cm^{-1} higher than that of ^{87}SrO and 0.97 cm^{-1} higher than that of ^{86}SrO. The *P*(22) line is 0.17 cm^{-1} higher than that of ^{87}SrO, but 0.20 cm^{-1} lower than that of ^{86}SrO! The analysis of the minor isotopomer lines was much more difficult for SrO as compared to BaO.

Four hundred sixty-six lines from 10 bands of ^{86}SrO and 734 lines from 12 bands of ^{86}SrO are assigned and available electronically. The maximum *J* quantum number was 114 in the (1, 0) band for both isotopomers.

E. Fitting the Dunham Parameters for the Ground State

To avoid the effect of the perturbations in the *A* state, we treated the data as if they were "fluorescence series" from different excited rovibronic levels (*23*). No attempt was made to fit spectroscopic constants to the $A^1\Sigma^+$ energy levels and they were represented simply as term values to be varied in a least-squares fit. Good spectral constants of the unperturbed ground state can be obtained by this method, no matter what

TABLE 3
Spectral Constants (in cm^{-1}) for the Ground State of ^{88}SrO

Constant		^{88}SrO	^{87}SrO	^{86}SrO
$Y_{1,0}$	ω_e	653.30998(140)	653.8864510	654.4774956
$Y_{2,0}$	$-\omega_e x_e$	-3.85078(79)	-3.85757874	-3.86455558
$Y_{3,0}$	$\omega_e y_e$	$-2.009(17)\times10^{-2}$	-2.0143228×10^{-2}	-2.0197900×10^{-2}
$Y_{4,0}$	$\omega_e z_e$	$1.2837(160)\times10^{-3}$	1.2882369×10^{-3}	1.2929009×10^{-3}
$Y_{5,0}$	-	$-9.8(5)\times10^{-6}$	-9.84331×10^{-6}	-9.88788×10^{-6}
$Y_{0,1}$	B_e	0.33797196(12)	0.33856866602	0.33918100355
$Y_{1,1}$	$-\alpha_e$	$-2.15598(22)\times10^{-3}$	-2.16169225×10^{-3}	-2.16755938×10^{-3}
$Y_{2,1}$	γ_e	$-1.9746(99)\times10^{-5}$	-1.9815787×10^{-5}	-1.9887529×10^{-5}
$Y_{3,1}$	-	$2.82(15)\times10^{-7}$	2.832464×10^{-7}	2.845288×10^{-7}
$Y_{4,1}$	-	$1.758(73)\times10^{-8}$	1.767328×10^{-8}	1.776935×10^{-8}
$Y_{0,2}$	$-D_e$	$-3.61035(180)\times10^{-7}$	-3.62310975×10^{-7}	-3.63622716×10^{-7}
$Y_{1,2}$	$-\beta_e$	$-4.483(15)\times10^{-9}$	-4.502814×10^{-9}	-4.523201×10^{-9}
$Y_{2,2}$	-	$-7.00(47)\times10^{-11}$	-7.03714×10^{-11}	-7.07539×10^{-11}
$Y_{3,2}$	-	$1.091(48)\times10^{-11}$	1.097757×10^{-11}	1.104721×10^{-11}
$Y_{0,3}$	H_e	$-6.37(79)\times10^{-14}$	-6.40380×10^{-14}	-6.43861×10^{-14}
$Y_{1,3}$	-	$-1.46(4)\times10^{-14}$	-1.46904×10^{-14}	-1.47836×10^{-14}

Note. Uncertainties in parentheses correspond to 95% confidence limit uncertainties (about two standard deviations). The digits shown are determined by the systematic rounding by the DSParFit program. Extra digits are reported for the constants calculated for ^{87}SrO and ^{86}SrO.

interactions occur in the upper state. A program called DSParFit, written by Professor R. J. Le Roy (*26–28, 23*), was used for our fits. In the DSParFit program, each datum is weighted with the square of the reciprocal of the estimated uncertainty. Treated as independent parameters, the rovibronic energy levels of the perturbed upper state are also predicted. The output of the program is also a set of upper state energy levels that can be used to study the perturbations of the *A* state. The program can also perform a systematic rounding of the final results to give a set of spectral constants with a minimum number of digits.

The rovibrational energies of the $X^1\Sigma^+$ state from ^{88}SrO were represented by the conventional double Dunham expansion (*30*):

$$E(v, J) = \sum_{k,m} Y_{k,m}(v + \tfrac{1}{2})^k[J(J+1)]^m. \qquad [4]$$

The constants for the other isotopomers were calculated through their dependence on the reduced mass (*31*),

$$Y_{k,m} \propto \mu^{-(k+2m)/2} \qquad [5]$$

using $\mu(^{88}SrO) = 13.5325855994$, $\mu(^{87}SrO) = 13.5087352668$, and $\mu(^{86}SrO) = 13.4843473867$ (*29*). The DSParFit program fits the Dunham constants for a selected reference isotopomer and includes the other isotopomers through the isotopic relationship, Eq. [5]. Terms to account for the breakdown of the Born–Oppenheimer approximation can also be included but this was not necessary in the SrO case.

In this work, we selected ^{88}SrO as the reference isotopomer. The ^{87}SrO and ^{86}SrO isotopomers were included in fitting through the reduced mass relationship of Eq. [5]. To improve the fit, we included 29 microwave data and 43 infrared data from the literature (*9, 10*). The uncertainty of our data was set as 0.005 cm^{-1}, while that of the other high-resolution data was obtained from the original literature. A total of 10 247 data from 1317 upper energy levels (fluorescence series) in our experiment were used in the final fit. We selected the Dunham expansion of orders of 5, 4, 3 and 1, respectively, for the $Y_{k,0}$, $Y_{k,1}$, $Y_{k,2}$, and $Y_{k,3}$ parameters.

In the final fit, a total of 1333 parameters were obtained: 16 Dunham constants and 1317 rovibrational energy levels for the *A* state. The dimensionless standard deviation of the fit was 1.49 when all our data were fixed at the uncertainty of 0.005 cm^{-1}. The Dunham constants we obtained for ^{88}SrO are listed in Table 3. The derived spectral constants from Eq. [5] for the ^{87}SrO and ^{86}SrO isotopomers are shown in the same table. The experimental line positions, together with the observed minus calculated values, and the fitted upper state rovibrational energies are available electronically.

IV. CONCLUSION

We have analyzed the $A^1\Sigma^+$–$X^1\Sigma^+$ chemiluminescence spectrum of SrO using a Fourier transform spectrometer. A total of 75 bands from three isotopomers were measured for vibrational lev-

els of the ground state up to $v'' = 12$. Over 10 000 rovibrational lines were assigned with a maximum J value as high as 153. An improved set of Dunham constants for the ground state was derived from a least-squares fitting of our data, along with microwave data and infrared data from the literature. For the upper A state, vibrational levels were detected for $v' = 0$ to $v' = 8$ and many new perturbations were observed.

ACKNOWLEDGMENTS

This work was supported by the National Sciences and Engineering Research Council of Canada (NSERC). Partial support was also provided by the Petroleum Research Fund of the American Chemical Society. We thank Professor Robert J. Le Roy for helpful discussions and for providing the DSParFit program.

REFERENCES

1. R. Mecke and M. Guillery, *Phys. Z.* **28,** 514–531 (1928).
2. J. Querbach, *Z. Phys.* **60,** 109 (1930).
3. K. Mahla, *Z. Phys.* **81,** 625 (1933).
4. W. F. Meggers, *Bur. Stand. J. Res.* **10,** 669 (1933).
5. G. Almkvist and A. Lagerqvist, *Ark. Fys.* **1,** 477–494 (1949).
6. G. Almkvist and A. Lagerqvist, *Ark. Fys.* **2,** 233–251 (1950).
7. V. A. Lagerqvist and L. Selin, *Ark. Fys.* **11,** 323–328 (1956).
8. M. Kaufman, L. Wharton, and W. Klemperer, *J. Chem. Phys.* **43,** 943–952 (1965).
9. W. H. Hocking, E. F. Pearson, R. A. Creswell, and G. Winnewisser, *J. Chem. Phys.* **68,** 1128–1134 (1978).
10. C. E. Blom, H. G. Hedderich, F. J. Lovas, R. D. Suenram, and A. G. Maki, *J. Mol. Spectrosc.* **152,** 109–118 (1992).
11. R. W. Field, *J. Chem. Phys.* **60,** 2400–2413 (1974).
12. G. A. Capelle, H. P. Broida, and R. W. Field, *J. Chem. Phys.* **62,** 3131–3136 (1975).
13. J. Hecht, *J. Chem. Phys.* **65,** 5026–5027 (1976).
14. R. Skelton, H. Li, C. Focsa, B. Pinchemel, and P. F. Bernath, unpublished manuscript.
15. R. F. W. Herrmann, G. K. Sumnicht, M. Stein, and W. E. Ernst, *J. Mol. Spectrosc.* **156,** 487–500 (1992).
16. P. F. Bernath, *Science* **254,** 665–670 (1991).
17. P. F. Bernath, *Adv. Photochem.* **23,** 1–61 (1997).
18. A. Lagerqvist and I. Renhorn, *J. Mol. Spectrosc.* **87,** 300–301 (1981).
19. T. Hirao, B. Pinchemel, and P. F. Bernath, *J. Mol. Spectrosc.*, in press.
20. B. Edlén, *Metrologia* **2,** 71–80 (1966).
21. K. P. Birch and M. J. Downs, *Metrologia* **30,** 155–162 (1993).
22. G. Norlén, *Phys. Scr.* **8,** 249–268 (1973).
23. H. Li, C. Focsa, B. Pinchemel, R. J. LeRoy, and P. F. Bernath, *J. Chem. Phys.*, in press.
24. F. W. Loomis and R. W. Wood, *Phys. Rev.* **32,** 223 (1928).
25. L. Gerö, *Z. Phys.* **93,** 669 (1935).
26. R. J. Le Roy, *J. Mol. Spectrosc.* **194,** 189–196 (1999).
27. R. J. Le Roy, *J. Mol. Spectrosc.* **191,** 223–231 (1998).
28. C. Fosca, H. Li, and P. F. Bernath, *J. Mol. Spectrosc.* **200,** 104–119 (2000).
29. I. Mills, T. Cvitaš, K. Homann, N. Kallay, and K. Kuchitsu, "Quantities, Units and Symbols in Physical Chemistry (International Union of Pure and Applied Chemistry)," 2nd ed., Blackwell Scientific, Oxford, 1993.
30. J. L. Dunham, *Phys. Rev.* **41,** 721–731 (1932).
31. P. F. Bernath, "Spectra of Atoms and Molecules," Oxford University Press, New York, 1995.